INTEGRATED HIGH-POWER TESTS OF DRESSED N-DOPED 1.3 GHz SRF CAVITIES FOR LCLS-II

N. Solyak#, T. Arkan, B. Chase, A. Crawford, E. Cullerton, I. Gonin, A. Grassellino, C. Grimm, A. Hocker, J. Holzbauer, T. Khabiboulline, O. Melnychuk, J. Ozelis, T. Peterson, Y. Pischalnikov, K. Premo, A. Romanenko, A. Rowe, W. Schappert, D. Sergatskov, R. Stanek, G. Wu,
FNAL, Batavia, IL 60510, USA

Abstract

New auxiliary components have been designed and fabricated for the 1.3 GHz SRF cavities comprising the LCLS-II linac. In particular, the LCLS-II cavity's helium vessel, high-power input coupler, higher-order mode (HOM) feedthroughs, magnetic shielding, and cavity tuning system were all designed to meet LCLS-II specifications. Integrated tests of the cavity and these components were done at Fermilab's Horizontal Test Stand (HTS) using several kilowatts of continuous-wave (CW) RF power. The results of the tests are summarized here.

INTRODUCTION

The LCLS-II 4 GeV superconducting linac [1] is based on XFEL/ILC technology intensively developed over the last couple of decades. A major difference however is that LCLS-II operates in the CW regime, whereas the XFEL/ILC will operate in pulsed mode. This required modifications to or complete re-design of some of the basic components: cavity Helium vessel, tuner, power coupler, and other cryomodule parts in order to accommodate the much higher cryogenic loads expected in the CW regime. To accelerate the production of two pre-production cryomodules, it was decided to use existing ILC bare cavities and fundamental power couplers, which led to some constraints.

The major LCLS-II modifications of the dressed cavity and auxiliaries are as follows:

- Nitrogen doped cavity to reduce losses in CW regime. LCLS-II requirements: $Q_0 > 2.7 \times 10^{10}$ at the nominal gradient of 16 MV/m.
- Helium vessel with a larger diameter two-phase connection to accommodate higher heat flux, and two helium supply inlets to provide more uniform thermal gradients during cooldown, which are crucial to effective magnetic flux expulsion, and hence low surface resistance.
- Two layers of magnetic shielding to reduce residual magnetic field at the cavity below 5mG.
- New end-lever tuner design which had to remain compatible with the "short-short" version of the ILC cavity adopted for the pre-production cryomodule. This design must also fit the "short-long" XFEL version of the cavity, which was adopted for production cryomodules.
- Design of the fundamental power coupler (FPC) was modified to fulfil LCLS-II requirements: loaded Q=4 x 10^7 and average power up to 6.4kW (includes 1.6kW of reflected power). Major modifications include reduction of the antenna length by 8.5mm and increase in the thickness of copper plating on the inner conductor of warm section to reduce coupler temperature.

To minimize the risks to the project all technical solutions and new designs have to be prototyped and tested in a cryomodule. Testing was focused on the most critical components and technical solutions, and performed in the Horizontal Test Stand cryostat (HTS) under conditions approximating the final cryomodule configuration. An integrated cavity test was the last stage of the design verification program. In this test a nitrogen doped cavity (AES021), previously qualified in a vertical cryostat, was dressed and fully assembled with all components (fundamental power coupler, two-layer magnetic shielding, XFEL-type feedthroughs, end-lever tuner). All components were previously individually tested in the HTS with cavities, but not as a complete integrated system. One major goal of this integrated test was to demonstrate that high Q_0 values demonstrated in vertical test can be preserved even when additional sources of heating from the power coupler and tuner and potential additional external magnetic fields from auxiliary components are present.

Other important studies related to design verification included thermal performance and power handling of the power coupler, heating of HOM couplers and tuner components, tuner performance, sensitivity to microphonics, and frequency control. Data from this test program allows component design to be verified and certain other aspects of cryomodule design (e.g., component thermal anchoring) to be finalized.

TEST PREPARATION AND CAVITY CONFIGURATION

Dressed cavity AES021 was tested previously in a vertical test stand (VTS) without HOM feedthroughs. HOM feedthroughs were later installed in a clean room and after a brief high pressure water rinse, a pumping manifold was installed, the cavity evacuated, and successfully leak checked. The cavity field probe was not removed or replaced. The cavity was transported to a different clean room for installation of the coupler cold section. No additional cleaning of the cavity surfaces took place either as part of or subsequent to coupler installation. HOM feedthroughs were later installed in a clean room and after brief high pressure water rinsing, a pumping manifold was installed and cavity was leak tight. Cavity was transported to assembly clean room for

solyak@fnal.gov

coupler installation. There was no cleaning work for the cavity during and after coupler installation.

The tuner [2] was installed with a pre-determined cavity compression/frequency offset. Two layers of Cryoperm® 10 magnetic shield were installed on the cavity. Magnetic shield end caps were comprised of a single layer and connected to the outer layer of the shield. Additional MetGlas® foil [3], a thin and flexible magnetic shield alloy, was used to cover the majority of the remaining openings in the magnetic shields. The coupler beam pipe port was left uncovered while the tuner-side beam pipe port was covered by the magnetic foil. Multi-layer insulation was placed between the inner and outer magnetic shields. The inside surfaces of the magnetic shields are covered with an insulating material (Kapton® tape) in order to electrically isolate them and minimize any potential thermal currents.

The remnant magnetic fields of all components (e.g., tuner, feedthroughs, etc.) were measured at a distance of 2" with a 3-D magnetometer and demagnetized if needed before they were attached to the cavity. All fields were found to be less than 5mG with the exception of the tuner motor. Since it was located at least 10" away from the cavity, it was not magnetically shielded.

Thermal straps were attached to the cavity beam pipes next to the end flanges. The two HOM feedthroughs were also thermally strapped. These thermal straps were then connected to the 2K two phase helium pipe when the cavity was installed in the HTS cryostat. Apiezon® grease was used to ensure good thermal conduction between the copper fixtures and the clamping surfaces. The power coupler 5K thermal intercept is a specialized design utilizing high purity aluminum and OFHC copper. The coupler 50 K thermal shield flange was connected to the cryostat's 80K thermal shield using a commercially procured high purity copper braid. The slow tuner motor housing was thermally strapped to the cryostat's 5K shield (see Figure 1).

Figure 1: The coupler side of TB9AES021 showing two layers of magnetic shields, MLI, HOM feedthrough thermal straps and the vacuum manifold.

The beam pipe flange at the field probe/tuner side of the cavity was sealed with NbTi blank. The beam pipe at the coupler side of the cavity was sealed with a 316SS flange that comprises a vacuum manifold which connects the cavity to the cryostat clean pumping system. The cavity was actively evacuated during testing. The cryostat insulating space was evacuated to 1 x 10^{-6} Torr, and leak checked, before cooldown commenced.

DIAGNOSTICS

In order to extract as much performance information as possible for this integrated test, the cavity and coupler were extensively instrumented with thermometers. A total of 17 RTDs were mounted onto the cavity itself. These included 6 RTDs mounted inside the helium vessel on the cavity cells, 4 RTDs mounted on the cavity beam pipes (external to the helium vessel), and 6 RTDs mounted on each of the HOM assemblies. In addition an RTD was mounted on the tuner-end NbTi beampipe flange, to detect any RF heating on the end flange (see Figure 2).

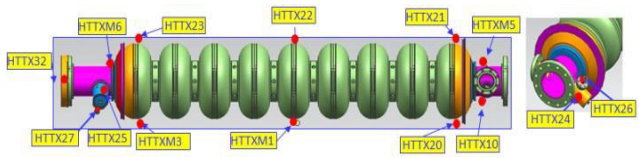

Figure 2: Cavity temperature sensors.

The fundamental power coupler had 15 thermal sensors (Cernox, platinum, and IR sensors) to measure and monitor coupler temperatures (see Figure 3). These sensors are attached to the 2K, 5K, 80K, and 300K sections of the coupler in addition to 5K and 80K thermal straps. The IR sensors monitor the warm window and warm inner conductor temperatures. In addition to thermal sensors, the coupler is equipped with electron pickups to monitor electron activity at the 5K and 80K windows that may be present due to multipacting or RF breakdown.

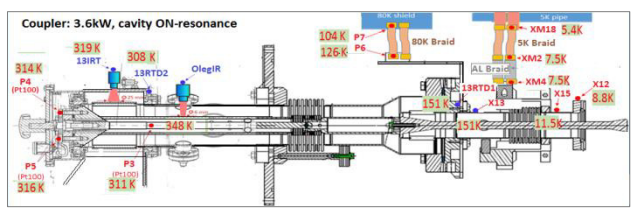

Figure 3: power coupler temperature diagnostics. Temperature map is shown for 3.6 kW of power measured for AES021 cavity in integrated test.

A total of 4 fluxgate sensors were mounted on the cavity. Two were mounted inside the Helium vessel (hence inside the cavity magnetic shielding) on the walls of cell #1, and oriented in such a way as to detect the axial and tangential field components. The other two sensors were mounted on the beam pipes, to measure axial field components outside of the magnetically shielded volume. This combination of sensors allowed measurements of ambient magnetic field on the cavity walls before, during, and after the superconducting

ISBN 978-3-95450-178-6

transition, providing an estimate of the effectiveness of both magnetic shielding and flux expulsion during cooldown.

FUNDAMENTAL POWER COUPLER PERFORMANCE

The warm section of the power coupler was assembled on the cavity after it was installed in the HTS. A portable clean room was used to eliminate particle contamination. After connection, the coupler vacuum space was evacuated.

Coupler thermal intercepts, comprising short flexible copper braids (commercially sourced from TAI) were installed to provide passive cooling of the coupler. F Two braids connected a copper can attached to the coupler CF100 flange (functioning as a 70K intercept) to the cryostat's 80K shield. The other two braids connected the 5K coupler intercept to the 5K thermal shield of HTS. These copper braids were extended by adding two straps made of pure aluminium (AL5N, each 95mm long, with a cross section of 125mm^2). Figure 4 shows details of the coupler thermal connection at 80K and 5K coupler ends.

Figure 4: Coupler thermal 70K (left) and 5K connection.

Power conditioning was initially performed at 300K before HTS cool down. The maximum RF power was limited to 6kW. During conditioning coupler vacuum level was limited to 6 x 10^{-7} Torr, while RF power was increased gradually from 4.5 to 6 kW. Total processing time (until thermal equilibrium was reached) was about 9.5 hours.

During RF power processing the cryostat was open to air to provide better cooling conditions. The maximum temperature detected on the inner conductor of the warm section of the coupler was about 400F, as shown in Figure 5. No breakdown or multipacting was observed in the coupler during HTS testing.

After cool-down of the cavity to a nominal temperature of 2K, coupler conditioning continued with the cavity off-resonance. In this regime power dissipation and temperature in the coupler was lower compared to the cavity on-resonance case, as predicted in simulations. In earlier tests the coupler was conditioned up to 6 kW, but in the current test we did tto exceed 4 kW of RF power.

Finally, the coupler was tested with the cavity on-resonance with up to 4kW forward power, which produces the same heat load as the LCLS-II most stringent requirements at 0.3mA beam current operation: 6.4 kW of forward power with 1.6kW reflected power (total 8kW) and a Q_{ext} of 4 x 10^7. Figure 6 shows the results from about 1.5 days of coupler tests at different power levels. The plot presents power level, vacuum and temperatures in warm parts of the coupler. Temperatures in the cold sections are summarized in Figures 7 and 8.

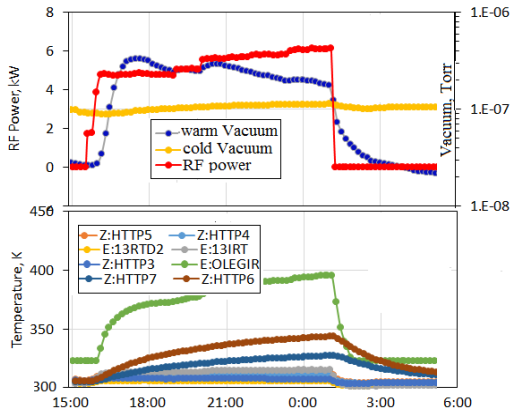

Figure 5: Power coupler warm conditioning. Upper plot shows RF power (red); vacuum in warm (blue) and cold (yellow) sections. Temperatures at different locations vs. RF power is shown in the bottom plot.

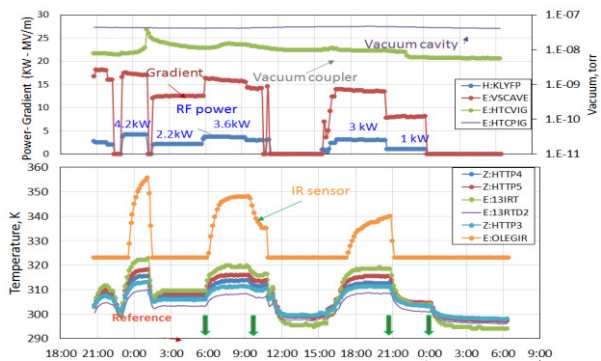

Figure 6: Coupler tested at different RF powers. Top plot shows RF power, accelerating gradient and vacuum in warm section of FPC. Bottom plot shows temperature on warm part of the coupler.

Temperatures on the CF100 flange and both ends of the 70K thermal braids (source and sink) are shown in Figure 7. Differential temperature on the copper braid (P7-P6) was used to estimate power flux, shown on the right plot in Figure 7. We estimated the RRR of the copper to be 100 from manufacturer's data; no empirical measurement of RRR was available.

Figure 8 (left) shows temperature versus RF power for different sensors on the 5K end of the coupler. The temperature drops across the AL6061aluminium can and on the copper braid were used to estimate power flux at 5K. For a RRR of 30 for the copper braid, both estimations agree and are consistent with results of thermal simulations. Copper braid thermal conduction and RRR will be measured at 5K in a LHe Dewar to verify our estimates and refine real power flux measurements.

Based on these test results, the design of the coupler thermal anchoring in the LCLS-II cryomodule was finalized.

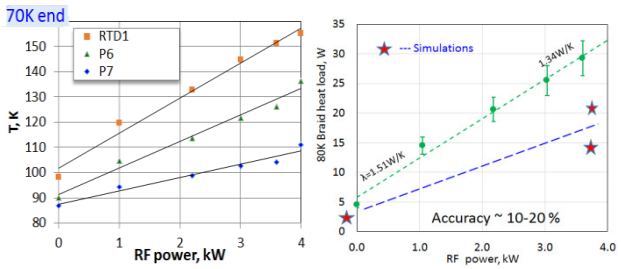

Figure 7: Temperature vs. RF power measured at the 70K intercept (cavity on-resonance). Power flux recalculated from temperature difference on the copper braids (green), simulations are shown in blue.

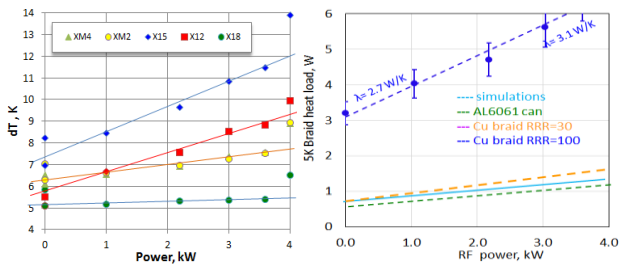

Figure 8: 5K intercept. Temperature vs. RF power (left) and recalculated power flux going to 5K thermal shield.

CAVITY Q_0 MEASUREMENTS

Final Q_0 measurements were performed after a standardized fast cool down procedure. After the cavity and cryostat were held at 3K for more than three weeks, the cavity temperature was raised to an average of 45 K. With the LHe supply pressure at 24 psig the supply valve was fully opened and two-phase LHe at 5 g/sec flowed into the two inlets of the cavity helium vessel, passing across he cavity cells and was exiting through the helium two phase return pipe (2K header). This created a vertical cavity temperature gradient of between 7K and 22 K during the superconducting transition. This thermal gradient expelled the magnetic flux successfully as seen on the fluxgate magnetometers. Figure 9 shows the cavity temperature and the magnetometer reading during the fast cool down.

Determination of cavity Q_0 requires the measurement of accelerating gradient and power dissipation in the cavity walls. Cavity dynamic heat load (power dissipation) was calculated by calorimetrically measuring the heat load in the 2K He bath via a mass flowmeter. A heater in the 2K header was used to provide a calibration between mass flow and power dissipated in the He bath. As the cavity was operated at various accelerating gradients, the 2K mass flow was measured and cavity heat load thus calculated. Figure 10 shows mass flow during the cavity dynamic heat load measurement.

Cavity gradient was determined using two different methods, measurement of cavity transmitted power along with knowledge of the external Q of the field probe (Q_2), or by measurement of forward power along with knowledge of the power coupler external Q (Q_1). Q_2 can be measured in the HTS using a network analyzer or values previously measured during vertical testing can be used if the field probe was not changed. The external Q of the coupler (Q_1) was obtained by measuring cavity power decay (loaded-Q measurement). The two methods agreed to within 5%. In Figure 11 the results of Q_0 measurements are plotted, using the average of the two methods to determine gradient.

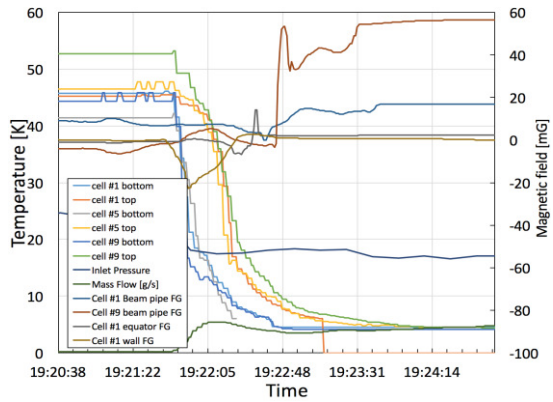

Figure 9: Cavity temperatures and magnetometer readings during the fast cool down.

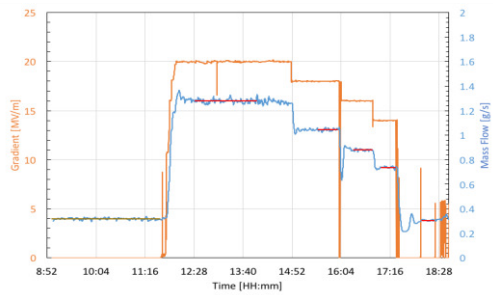

Figure 10: Dynamic heat load measurement.

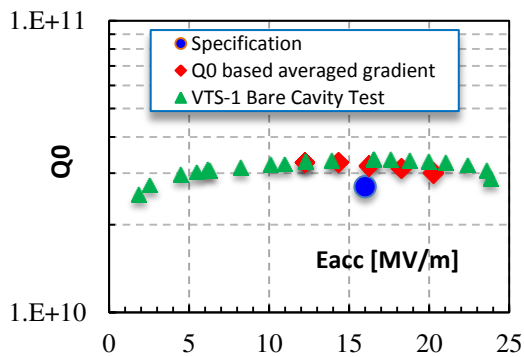

Figure 11: Cavity Q vs. E_{acc} during bare cavity vertical test and horizontal integrated test.

HOM COUPLER HEATING

To dissipate heat generated in the HOM antenna and in the HOM cables, the HOM feedthrough is thermally anchored to the 2K two-phase helium pipe by double thermal strap. Temperatures on both ends of these straps and on the HOM body between the two formteil legs were measured for different accelerating gradients up to 20

ISBN 978-3-95450-178-6

MV/m. Figure 12 shows HOM power and temperature on the HOM body and feedthrough as a function of cavity gradient. The maximum power in the HOM coupler (leakage of fundamental mode) was about 50mW; the temperature increase at 20MV/m was also small < 0.2 K.

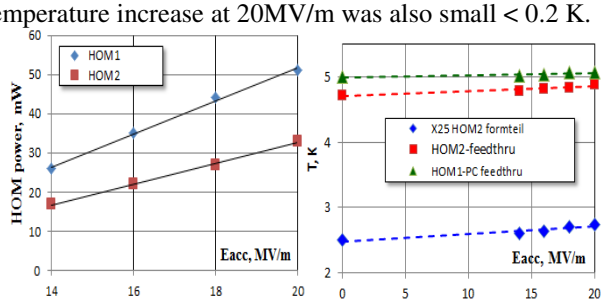

Figure 12: HOM rf power (left) and heating (right) vs. accelerating gradient in cavity.

At the beginning of this test multipacting was observed in HOM2 (tuner side) at ~8MV/m, but it disappeared after a brief period of processing. Simulations confirm the probability to have multipacting at this gradient [4].

TUNER PERFORMANCE, MICROPHONICS AND FREQUENCY CONTROL

During the integrated test of AES021 (and subsequently AES028) dedicated studies of the cavity tuner were conducted. A primary goal was to confirm performance parameters of the tuner as measured in previous tests with dressed cavities [2]. Results of tuner performance are summarized in Table 1.

Table 1: LCLS II SRF Cavity Tuner Parameters

Tuner parameters	*specifications*	*measured*
Coarse Tuner ration	20	21.5
Coarse Tuner frequency max. range	450kHz	>600kHz
Coarse Tuner resolution	1-2 Hz/step	1.3Hz/step
Coarse Tuner short range hysteresis	50Hz	45Hz
Piezo Tuner range(for 4 piezo & 120V)	1kHz	3kHz
Piezo Tuner Resolution	1Hz	0.1Hz

The minimum and maximum range of the coarse tuner was determined by first using the tuner to put the cavity in the "relaxed" (un-loaded) position (see Figure 13).

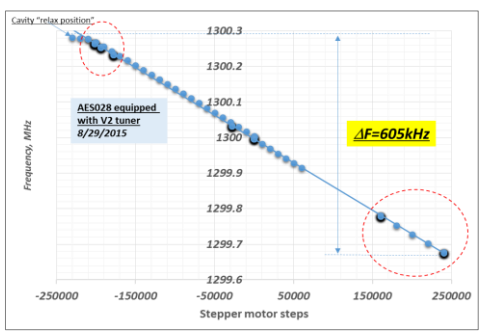

Figure 13: Cavity frequency change by coarse tuner/stepper motor.

The cavity was then compressed with the low tuner. Piezo tuner hysteresis (cavity frequency shift versus voltage applied to piezo) was measured at different values of the cavity frequency. Results indicate that the piezo response is practically flat (22.8±0.7 Hz/V) starting from ΔF = 20 kHz up to maximum ΔF = 600 kHz.

The effect of cavity detuning due to microphonics was studied with and without piezo compensation [5]. The piezo-stack was driven with a combination of the signals: feed-forward proportional to E^2_{acc} to compensate Lorentz Force detuning, slow feedback for cavity detuning, and 45Hz single resonance suppression. Summary of the active resonance control on cavity with piezo tuner is shown in Figure 14.

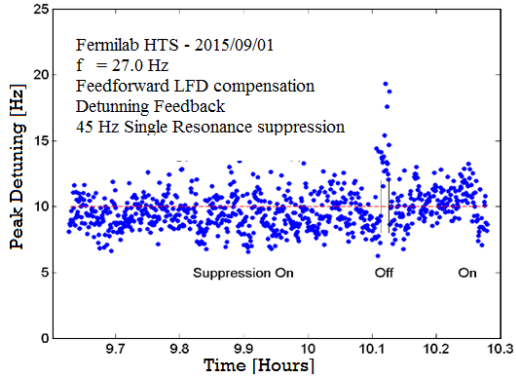

Figure 14: Active Resonance Control of the AES028 with piezo-tuner. Red-line is LCLS II specifications.

CONCLUSION

The first integrated test at FNAL of a nitrogen doped high-Q cavity demonstrated that the cavity, assembled with components designed or modified to meet the requirements of the LCLS-II project, still exhibits the high-Q demonstrated in vertical test. It demonstrates that cavity dressing, assembly, and operation with all auxiliary components will not degrade cavity performance if done properly. Power coupler heating and performance in test closely matches expectations and the tuner design was verified.

ACKNOWLEDGMENT

We appreciate the contributions to this work and assistance from the LCLS-II teams at Fermilab, SLAC and JLAB.

REFERENCES

[1] J.Galayda, "The new LCLS-II project: Status and challenges", Linac14, Geneva, Switzerland.
[2] Y. Pischalnikov, *et al*. "Design and Test of Compact Tuner for Narrow Bandwidth SRF Cavities", IPAC2015, Richmond, VA, USA.
[3] G. Wu, et al., "Magnetic foils for SRF cryomodule" these proceedings, SRF'2015, Whistler, Canada.
[4] G.Romanov *et al*, "Multipactoring in ILC HOM coupler", TD-Note-15-16.
[5] W. Schappert *et al*. "Resonance Control for Narrow Bandwidth SRF Cavities", SRF2015, Whistler, BC, Canada.